Dynamic lane-changing trajectory planning for autonomous vehicles in mixed traffic

Zhen Wang[1,2], Jianquan Chen[1], Pengchao Liu[1], Bo Dai[1], Guanqun Wang[3],* and Zhilin Han[2]

[1] School of Information Engineering, Chang'an University, Xi'an, Shaanxi, China

[2] Shandong Tuoluo Electronic Technology Co., Ltd., Heze, Shandong, China

[3] School of Electronic Information Engineering, Xi'an Technological University, Xi'an, Shaanxi, China

* Correspondence author; E-mail: wangguanqun@xatu.edu.cn.

Abstract: This paper presents a novel dynamic lane-changing trajectory planning (DLCTP) model for autonomous vehicle (AV) running in the mixed traffic environment. The proposed model fully considers the dynamics of surrounding human-driven vehicles and can work on both straight and curved roads. The first step of the DLCTP model is to decide when and where to make the lane change based on the car-following model and safety constraints. Upon decision-making, an optimal lane-changing trajectory that accounts for safety, comfort, and efficiency is generated at each time step until the lane-changing procedure is completed. CarSim-Simulink based simulation platform and three typical traffic scenarios are applied to validate the proposed DLCTP model. Experimental results show that the proposed DLCTP model can generate smooth, safe, and comfort trajectories even in complex traffic situations. The proposed DLCTP model can be employed directly on real AVs because it is easy to implement and can adapt to complex traffic environments.

Keywords: autonomous vehicles; decision-making; lane-changing model; dynamic trajectory planning; mixed traffic

1. Introduction

Autonomous vehicles (AVs) have developed and applied recently [1–3]. Numerous businesses, including Waymo, Uber, and Tesla, have commenced AV field tests on public roads. The integration of mixed traffic, comprising AVs and human-driven vehicles (HVs), is an unavoidable development in the imminent future [4,5]. Consequently, collaboration between AVs and HVs is crucial in a mixed traffic setting. Lane changing represents a conventional cooperative scenario between AVs and HVs. Given the unpredictability of human driver actions, a comprehensive analysis of AV lane-changing movements in mixed traffic is essential, particularly for lane-changing trajectory planning, which directly influences safety of all traffic participants. Moreover, the ideal lane-changing path can

prevent potential collisions, enhance the intelligence of AVs, and alleviate traffic congestion [2,3,6,7].

Lane-changing behavior is generally classified into three categories: mandatory lane change, discretionary lane change, and random lane change [8,9,10]. Mandatory lane changes occur when automobiles must circumvent barriers, such as lane blockages or lane reductions, or when exiting the expressway. A discretionary lane shift transpires when drivers intend to acquire a speed advantage. Drivers frequently alter lanes to circumvent a sluggish car ahead. No explicit rule governs the random lane-changing behavior. A random lane shift may yield advantages for the subject vehicle or may not affect its current position. Numerous researchers have recently proposed various lane-changing models [11–13]. Car-following models and safety distance regulations are extensively utilized in rule-based lane-changing models [14–17]. Nie *et al.* present a decentralized cooperative framework for lane-changing decision-making [13]. The proposed framework comprises three modules: state prediction, candidate decision generation, and coordination. Additionally, the impact of the proposed model on traffic stability, efficiency, homogeneity, and safety is examined through a numerical simulation experiment. Game theory is utilized in lane-changing models. Yu *et al.* introduce a lane-changing model grounded in game theory that emulates human behavior through interactions with adjacent cars via turn signals and lateral maneuvers [18]. The lane-changing controller can acquire information and learn essential knowledge from real-time interactions utilizing the proposed model. Ali *et al.* formulate a mandatory lane-changing model grounded in game theory [19]. The proposed paradigm is applicable in both traditional and connected environments. Discrete-choice lane-changing models are extensively researched to replicate driver behavior in intricate traffic situations [20,21]. Suh *et al.* delineate lane-changing motion planning utilizing a synthesis of probabilistic and deterministic predictions for AVs in intricate driving scenarios [22]. The risk of lane changing is assessed through predicted time-to-collision and safety distance to ensure safety during lane change maneuvers. Zhang *et al.* propose a parameter decision framework [23]. The decision is articulated through essential parameters rather than specific behaviors. Furthermore, an innovative trajectory planning method is introduced within this framework. Zhang *et al.* utilize the nonlinear model predictive control method with terminal limitations, devoid of a predetermined path configuration, to enhance flexibility in lane-changing decisions [23]. Incentive-based lane-changing models seek to enhance the overall efficiency of traffic flow during the lane-changing procedure [24,25]. Kesting *et al.* present a comprehensive lane-changing model to establish rules for discretionary and forced lane changes. The value of a certain lane and the risks linked to lane changes are assessed based on longitudinal acceleration, which is computed using microscopic traffic models. Except for these standard models, numerous developing technologies, like support vector machine [26] and deep learning technologies, are also applied to design artificial intelligence-based lane-changing models [27,28]. Ye *et al.* presented a framework of lane-changing decision-making training and learning [29]. There are two basic aspects of the proposed framework: the deep reinforcement learning training program and the high-fidelity virtual simulation environment. To verify the framework on a more complicated environment, and

train a model capable of managing most of the traffic situations, the model is extended integrating car-following and lane-changing behaviors on a three-lane segment. Experiment results suggest that the extended model including car-following and lane-changing behaviors is a more efficient approach. All these studies have achieved a lot in AV lane change. However, these studies use the static planning method in which the statuses of adjacent HVs are considered to keep unchanging in the complete lane-changing procedure. However, in the real-world traffic situation, the speed and position of nearby HVs are changing dynamically, and the AV needs to adapt its speed and position proportionately to guarantee safety in real time. Although Yang *et al.* have presented a dynamic lane-changing trajectory planning (DLCTP) model based on the polynomial curve, the proposed model only considers two surrounding cars and can only work on a straight road [30]. The aforementioned drawbacks constrain the practical applicability of this paradigm.

This work introduces an innovative DLCTP model that comprehensively accounts for the dynamics of all adjacent HVs to address this research gap. Additionally, the intricate road environment, comprising the curved roadway and four adjacent heavy vehicles, is incorporated into the DLCTP model. The proposed DLCTP model has four primary steps: lane-changing decision, dynamic trajectory planning, safety limitations, and final trajectory generation. In the lane-changing decision phase, the AV determines the timing and location for initiating the lane-changing operation based on the real-time conditions of adjacent high-velocity vehicles. The cubic polynomial curve is utilized to create a dynamic, smooth lane-changing route from the present location to the destination. Subsequently, safety limitations are taken into account to enhance the generated trajectory, ensuring compliance with collision-avoidance and rollover-avoidance requirements. The ideal lane-changing trajectory is produced by reconciling comfort and efficiency.

The primary contributions of this study are as follows:

(a) Propose a model for dynamic lane-changing trajectory planning.

(b) The proposed model accounts for the dynamics of all adjacent high-velocity vehicles and curving roadways.

(c) The proposed approach is directly applicable to actual AV operations.

The subsequent sections of this work are structured as follows. Section 2 provides a comprehensive introduction to the AV DLCTP model. Section 3 delineates the experimental parameters for the simulation and analyzes the results of the experiments. Section 4 summarizes the entire text and addresses prospective research endeavors.

2. Dynamic lane-changing trajectory planning model

2.1. Notation list

To help readers better understand our proposed DLCTP model, Table 1 lists the major notations utilized in this paper.

Table 1. Notation of major variable used in this paper.

Symbol	Description
C	Vehicle length
$\mathcal{T}$	Time duration in the DLCTP model
t	Time instant, $t \in \mathcal{T}$
$\mathcal{M}$	Set of time steps in the DLCTP model
m	Time step, $m \in \mathcal{M}$
$\mathcal{N}$	Set of all vehicles considered in the DLCTP model, $\mathcal{N} := \{\text{AV}, \text{TPV}, \text{TFV}, \text{CPV}, \text{CFV}\}$
n	Vehicle number, $n \in \mathcal{N}$
τ_n	Reaction time of vehicle n
t_m^S	Lane change start time instant in the time step m
t_m^F	Lane change finish time instant in the time step m
$v_n(t)$	Speed of vehicle n at time t
$\alpha_n(t)$	Heading of vehicle n at time t
$x_n(t), y_n(t)$	Lateral and longitudinal position of vehicle n at time t
$a_n(t)$	Acceleration of vehicle n at time t
$a_n^L(t)$	Lateral acceleration of vehicle n at time t
a_n^{MAX}	Maximum lateral acceleration of vehicle n
b_n^{MAX}	Maximum deceleration of vehicle n
$L^P(m)$	Safe distance between AV and TPV in the time step m
$L^F(m)$	Safe distance between AV and TFV in the time step m
$k_0(m), k_1(m), k_2(m), k_3(m)$	Parameters of the cubic polynomial curve in the time step m
k_4, k_5	Parameters of the linearized car-following model
$\hat{a}_n(t_m)$	Target acceleration of AV when following vehicle n
g	Desired time gap when implementing car following

2.2. DLCTP model framework

This section provides a comprehensive introduction to the proposed DLCTP model. Figure 1 illustrates the four essential processes in the DLCTP model: lane-changing decision, dynamic trajectory planning, safety limitations, and final trajectory generation. The AV comprises four components: environmental perception, mission decision-making, trajectory planning, and motion control [31]. The proposed DLCTP constitutes a segment of the AV trajectory planning component. The entire model is initiated upon getting the lane-changing directive from the AV mission decision component. The states of adjacent high-velocity vehicles are taken into account while determining lane-changing decisions. Should the present conditions render the lane-changing move perilous (e.g., neighboring high-velocity vehicles are uncooperative with the subject vehicle's lane shift), the AV will modify its speed in anticipation of initiating the lane change in the subsequent time step. Upon determining the timing and location for the lane change, a trajectory from the present position to the destination is formulated during the dynamic trajectory generating phase. The produced trajectory is thereafter forwarded to the safety constraints optimization phase. Collision

avoidance and rollover prevention are implemented to enhance the calculated trajectory by modifying the end location of the AV during lane changes. Ultimately, efficiency and comfort are harmonized to produce the definitive lane-changing trajectory.
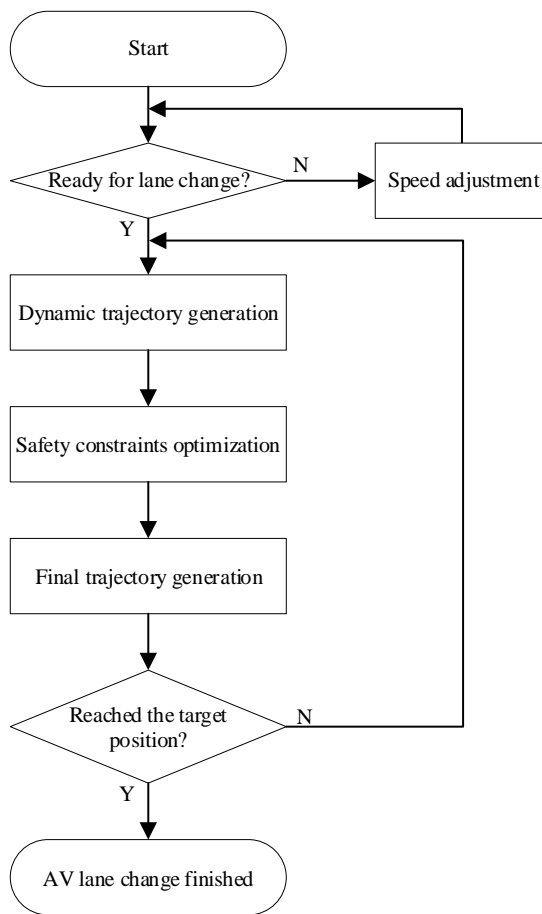

Figure 1. Framework of the proposed DLCTP model.

Prior to the AV attaining its ultimate position in the target lane, three phases are executed at each time interval: dynamic trajectory generation, optimization of safety limitations, and final trajectory generation. Figure 2a illustrates that the lane-changing process encompasses numerous time stages. To ensure safety, efficiency, and comfort during lane changes, the intended trajectory adjusts in accordance with the real-time conditions of surrounding high-velocity vehicles. Consequently, our proposed model can generate dynamic trajectories. Figure 2b depicts the final executed trajectory of the AV, corresponding to Figure 2a.
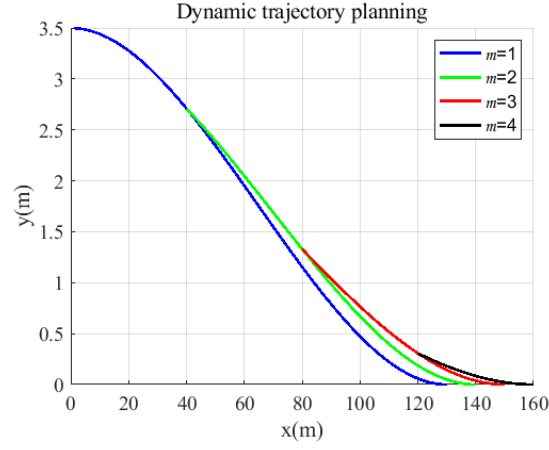
(a) Dynamic trajectory planning process.
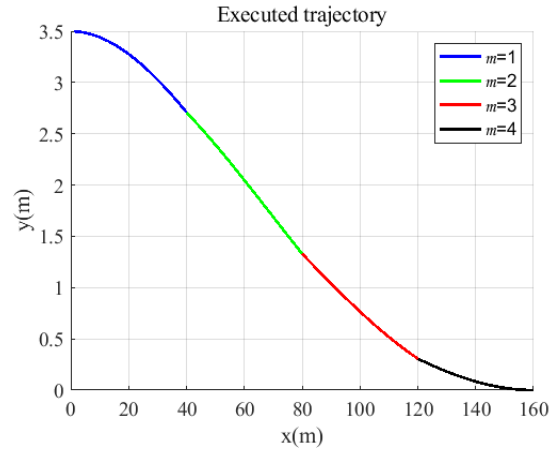
(b) Final executed trajectory.

Figure 2. Schematic of dynamic trajectory planning at different time step.

2.3. Dynamic lane-changing trajectory

The cubic polynomial function is utilized to depict the AV's lane-changing path in our model. This graph exhibits second-order smoothness, indicating that both the position and velocity of the AV remain constant throughout the lane-changing maneuver. Unlike higher-order polynomial functions, the cubic polynomial curve possesses fewer parameters, requiring less information to ascertain the function's parameters. The equation of the cubic polynomial curve is,

$$y_{AV}(x_{AV}(t)) = k_3(m)x_{av}(t)^3 + k_2(m)x_{AV}(t)^2 + k_1(m)x_{AV}(t) + k_0(m), \forall m \in M, t \in T \quad (1)$$

Assume the current states of surrounding HVs meet the lane-changing requirements (lane-changing decision is detailed depicted in Section 2.6), dynamic trajectory generation module will generate a trajectory from the current position $(x_{AV}(t_m^S), y_{AV}(t_m^S), \alpha_{AV}(t_m^S))$ to the target position $(x_{AV}(t_m^F), y_{AV}(t_m^F), \alpha_{AV}(t_m^F))$ (shown in Figure 3, vehicles and dashed vehicles denote the initial and final positions of all vehicles, respectively). AV's localization module is capable of providing position and heading information in real time. Target heading $\alpha_{AV}(t_m^S)$ can be obtained after getting the position and the high-definition map of the

environment [30]. To simplify the notations, the AV's dynamic coordinate is employed. Thus, for each time step m, there is,

$$x_{AV}(t_m^S) = 0, \forall m \in M, t \in T; \tag{2}$$

$$y_{AV}(t_m^S) = 0, \forall m \in M, t \in T; \tag{3}$$

$$y_{AV}(x_{AV}(t_m^S)) = y_{AV}(t_m^S), \forall m \in M, t \in T; \tag{4}$$

$$y_{AV}(x_{AV}(t_m^F)) = y_{AV}(t_m^F), \forall m \in M, t \in T; \tag{5}$$

$$y'_{AV}(x_{AV}(t_m^S)) = \tan(\alpha(t_m^S)), \forall m \in M, t \in T; \tag{6}$$

$$y'_{AV}(x_{AV}(t_m^F)) = \tan(\alpha(t_m^F)), \forall m \in M, t \in T. \tag{7}$$

Substituting Equations (2)–(7) into Equation (1), we can get the parameters,

$$k_0(m) = 0, \forall m \in M; \tag{8}$$

$$k_1(m) = \tan(\alpha(t_m^S)), \forall m \in M, t \in J; \tag{9}$$

$$k_2(m) = \frac{3y_{AV}(t_m^F) - x_{AV}(t_m^F)(\tan(\alpha_{AV}(t_m^F)) + 2\tan(\alpha_{AV}(t_m^S)))}{(x_{AV}(t_m^F))^2}, \forall m \in M, t \in T; \tag{10}$$

$$k_3(m) = \frac{x_{AV}(t_m^F)(\tan(\alpha_{AV}(t_m^F)) + \tan(\alpha_{AV}(t_m^S))) - 2y_{AV}(t_m^F)}{(x_{AV}(t_m^F))^3}, \forall m \in M, t \in T. \tag{11}$$

Substituting Equations (8)–(11) into Equation (1) can get the cubic lane-changing trajectory,

$$
\begin{aligned}
y_{AV}(x_{AV}(t_m)) = {} & \frac{x_{AV}(t_m^F)(\tan(\alpha_{AV}(t_m^F)) + \tan(\alpha_{AV}(t_m^S))) - 2y_{AV}(t_m^F)}{(x_{AV}(t_m^F))^3} x_{AV}(t_m)^3 + \\
& \frac{3y_{AV}(t_m^F) - x_{AV}(t_m^F)(\tan(\alpha_{AV}(t_m^F)) + 2\tan(\alpha_{AV}(t_m^S)))}{(x_{AV}(t_m^F))^2} x_{AV}(t_m)^2 + \\
& \tan(\alpha(t_m^S)) x_{AV}(t_m), \forall m \in M, t \in T.
\end{aligned}
\tag{12}
$$

In Equation (12), only the target position $(x_{AV}(t_m^F), y_{AV}(t_m^F), \alpha_{AV}(t_m^F))$ is unknown. However, with the help of the high-definition map [30], the final latitudinal position $y_{AV}(t_m^F)$ and heading $\alpha_{AV}(t_m^F)$ can be acquired easily after getting the final longitudinal position $x_{AV}(t_m^F)$. As a result, the lane-changing trajectory in each time step is uniquely determined by the final longitudinal position $x_{AV}(t_m^F)$.

Many critical factors, including comfort and efficiency, should be put into consideration when planning the lane-changing trajectory. However, there is a conflict between these two key factors. A cost function is constructed to evaluate how comfort and efficiency affect the optimal trajectory planning. Equation (13) is the constructed cost function.

$$J = \delta a_{AV}^L(t_m^F) + (1 - \delta)(t_m^F - t_m^S), \forall \delta(0,1), m \in M, t \in T. \tag{13}$$

In Equation (13), the lateral acceleration reaches a maximum at the final position of the planned trajectory [32]. As a result, the lateral acceleration is employed to represent the comfort for passengers during the lane change. The lane-changing efficiency is evaluated based on the lane-changing's duration. The longer time means lower efficiency.

Moreover, with the help of centrifugal force equation, the lateral acceleration at the final position can be calculated by Equation (14),

$$a_{AV}^L(t_m^F) = (v_{AV}(t_m^F))^2 F(x_{AV}(t_m^F)), \forall m \in M, t \in T. \tag{14}$$

$F(x_n(t_m))$ denotes the curvature function of vehicle n in the time step m during the lane change. $F(x_n(t_m))$ can be obtained from Equation (15),

$$f(x_n(t_m)) = \left| \frac{y_n^{\prime\prime}(t_m)}{(1 + y_n^{\prime}(t_m))^{\frac{3}{2}}} \right|, \forall m \in M, n \in N, t \in T. \tag{15}$$

In Equation (15), $y_n^{\prime}(t_m)$ and $y_n^{\prime\prime}(t_m)$ are the first and second derivatives of the lane-changing trajectory equation, respectively, which are listed as follows,

$$y_n^{\prime}(t_m) = \frac{3x_{AV}(t_m^F)(\tan(\alpha_{AV}(t_m^F)) + \tan(\alpha_{AV}(t_m^S))) - 6y_{AV}(t_m^F)}{(x_{AV}(t_m^F))^3} x_{AV}(t)^2 +$$
$$\frac{6y_{AV}(t_m^F) - 2x_{AV}(t_m^F)(\tan(\alpha_{AV}(t_m^F)) + 2\tan(\alpha_{AV}(t_m^S)))}{(x_{AV}(t_m^F))^2} x_{AV}(t) + \tag{16}$$
$$\tan(\alpha_{AV}(t_m^S)), \forall m \in M, t \in T;$$

$$y_n^{\prime\prime}(t_m) = \frac{6x_{AV}(t_m^F)(\tan(\alpha_{AV}(t_m^F)) + \tan(\alpha_{AV}(t_m^S))) - 12y_{AV}(t_m^F)}{(x_{AV}(t_m^F))^3} x_{AV}(t) +$$
$$\frac{6y_{AV}(t_m^F) - 2x_{AV}(t_m^F)(\tan(\alpha_{AV}(t_m^F)) + 2\tan(\alpha_{AV}(t_m^S)))}{(x_{AV}(t_m^F))^2}, \forall m \in M, t \in T; \tag{17}$$

Substituting Equations (16) and (17) into Equation (15) produces,

$$F(x_n(t_m)) = \left| \frac{\dfrac{6x_{AV}(t_m^F)(\tan(\alpha_{AV}(t_m^F)) + \tan(\alpha_{AV}(t_m^S))) - 12y_{AV}(t_m^F)}{(x_{AV}(t_m^F))^3} x_{AV}(t) + \dfrac{6y_{AV}(t_m^F) - 2x_{AV}(t_m^F)(\tan(\alpha_{AV}(t_m^F)) + 2\tan(\alpha_{AV}(t_m^S)))}{(x_{AV}(t_m^F))^2}}{\left(1 + \left(\begin{array}{l} \dfrac{3x_{AV}(t_m^F)(\tan(\alpha_{AV}(t_m^F)) + \tan(\alpha_{AV}(t_m^S))) - 6y_{AV}(t_m^F)}{(x_{AV}(t_m^F))^3} x_{AV}(t)^2 + \\ \dfrac{6y_{AV}(t_m^F) - 2x_{AV}(t_m^F)(\tan(\alpha_{AV}(t_m^S)))}{(x_{AV}(t_m^F))^2} x_{AV}(t) + \tan(\alpha(t_m^S)) \end{array}\right)^2\right)^{\frac{3}{2}}} \right|, \tag{18}$$
$$\forall m \in M, t \in T$$

After arriving the final position, the curvature of AV is,

$$F(x_n(t_m^F)) = \left| \frac{2x_{AV}(t_m^F)(2\tan(\alpha_{AV}(t_m^F)) + \tan(\alpha_{AV}(t_m^S))) - 6y_{AV}(t_m^F)}{(x_{AV}(t_m^F))^2(1 + \tan(\alpha_{AV}(t_m^F)))^{\frac{3}{2}}} \right|, \tag{19}$$
$$\forall m \in M, t \in T.$$

Replacing $F(x_n(t_m^F))$ in Equation (14) with Equation (19) produces,

$$\alpha_{AV}^L(t_m^F) = (v_{AV}(t_m^F)^2) \left| \frac{2x_{AV}(t_m^F)(2\tan(\alpha_{AV}(t_m^F)) + \tan(\alpha_{AV}(t_m^S))) - 6y_{AV}(t_m^F)}{(x_{AV}(t_m^F))^2(1 + \tan(\alpha_{AV}(t_m^F)))^{\frac{3}{2}}} \right|, \tag{20}$$
$$\forall m \in M, t \in T.$$

The final cost function J is listed as follows,

$$J = \delta((v_{AV}(t_m^F)^2) \left| \frac{2x_{AV}(t_m^F)(2\tan(\alpha_{AV}(t_m^F)) + \tan(\alpha_{AV}(t_m^S))) - 6y_{AV}(t_m^F)}{(x_{AV}(t_m^F))^2(1 + \tan(\alpha_{AV}(t_m^F)))^{\frac{3}{2}}} \right| + \tag{21}$$

$$(1-\delta)(t_m^F - t_m^S), \forall m \in M, t \in T.$$

Minimizing the cost function J to find the optimal lane-changing trajectory can produce the optimal final position of the AV. In other words, the optimal lane-changing trajectory is decided by the speed of AV $v_{AV}(t_m^S)$ and the weight factor δ.
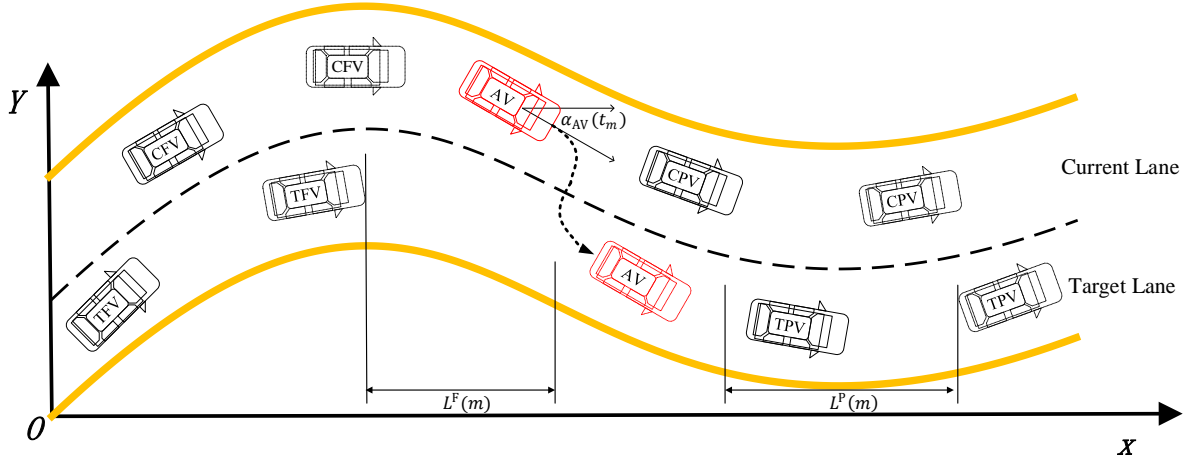

Figure 3. Schematic of the lane-changing process.

2.4. Safety constraints

In addition to comfort and efficiency, safety, encompassing collision avoidance and rollover prevention, must also be factored into the planning of the lane-changing trajectory. Figure 3 illustrates a typical lane-changing scenario involving four adjacent vehicles in both the current and target lanes. At each time step of lane-changing trajectory planning, the AV must sustain a safe distance from both the target lane's preceding vehicle (TPV) and the following vehicle (TFV). A safe distance regulation is established to determine the safe distance [33]. The safe distance rule ensures that the following vehicle maintains an adequate spacing from the preceding vehicle, preventing a rear-end collision in the event of an emergency stop by the latter. As shown in Figure 3, the safe distance between the TPV and the TFV in the lane-changing maneuver is $(x_{TFV}(t_m) + L^F(m), x_{TPV}(t_m) - C - L^P(m))$. One indicator to ensure that the AV will not crash during lane change is that the final position when reaching the center line of the target lane is within this position range. The reaction time τ_n of vehicle n is also considered in the safe distance rule. The safe distance is acquired based on the following equation,

$$L^P(m) = v_{AV}(t_m^S)\cos(\alpha_{AV}(t_m^S))\tau_{AV} + (v_{AV}(t_m^S)cos(\alpha_{AV}(t_m^S)) -$$

$$v_{TPV}(t_m^S)cos(\alpha_{TPV}(t_m^S)))(t_m^F - t_m^S) + \frac{1}{2}(a_{AV}(t_m^S)\cos(\alpha_{AV}(t_m^S)) - \tag{22}$$

$$a_{TPV}(t_m^S)\cos(\alpha_{TPV}(t_m^S)))(t_m^F - t_m^S)^2, \forall t \in T, m \in M;$$

$$L^F(m) = v_{TFV}(t_m^S)\cos(\alpha_{TFV}(t_m^S))\tau_{TFV} + (v_{TFV}(t_m^S)\cos(\alpha_{TFV}(t_m^S)) -$$

$$v_{AV}(t_m^S)\cos(\alpha_{AV}(t_m^S)))(t_m^F - t_m^S) + \frac{1}{2}(a_{TFV}(t_m^S)\cos(\alpha_{TFV}(t_m^S)) - \tag{23}$$

$$a_{AV}(t_m^S)\cos(\alpha_{AV}(t_m^S)))(t_m^F - t_m^S)^2, \forall t \in T, m \in M.$$

The ultimate positions of both TPV and TFV are essential for determining the safe positional range of the AV. Given that each time step is very brief (100 milliseconds), it is plausible to assume the TPV and TFV maintain a unchanging speed throughout every interval. Consequently, their ultimate positions can be determined using the following equations,

$$x_{TPV}\left(t_m^F\right) = x_{TPV}\left(t_m^S\right) + v_{TPV}\left(t_m^S\right)\cos\left(\alpha_{TPV}\left(t_m^S\right)\right)\left(t_m^F - t_m^S\right) \tag{24}$$

$$x_{TFV}\left(t_m^F\right) = x_{TFV}\left(t_m^S\right) + v_{TFV}\left(t_m^S\right)\cos\left(\alpha_{TFV}\left(t_m^S\right)\right)\left(t_m^F - t_m^S\right) \tag{25}$$

$$t_m^F - t_m^S = \frac{\int_0^{x_{AV}\left(t_m^F\right)}\sqrt{1 + (y'_{AV}\left(t_m^F\right))^2}}{v_{AV}\left(t_m^S\right)\cos\left(\alpha_{AV}\left(t_m^S\right)\right)} \tag{26}$$

Therefore, the safe distance for the AV's final position on the target lane is calculated based on the following equation,

$$x_{TFV}\left(t_m^S\right) + v_{TFV}\left(t_m^S\right)\cos\left(\alpha_{TPV}\left(t_m^S\right)\right)\left(t_m^F - t_m^S\right) + L^F(m), x_{TPV}\left(t_m^S\right) +$$

$$v_{TPV}\left(t_m^S\right)cos\left(\alpha_{TFV}\left(t_m^S\right)\right)\left(t_m^F - t_m^S\right) - L^P(m) - C) \tag{27}$$

In addition to collision-avoidance, rover-avoidance is also necessary when planning the lane-changing trajectory. To avoid a rover, the critical issue is to guarantee the lateral acceleration of AV reaching the lane-changing's destination should not exceed the threshold a_n^{MAX} [34]. According to Equation (14),

$$a_{AV}^L\left(t_m^F\right) = \left(v_{AV}\left(t_m^F\right)\right)^2 F\left(x_{AV}\left(t_m^F\right)\right) < a_n^{MAX} \tag{28}$$

Substituting Equation (19) into Equation (28), we can get,

$$x_{AV}\left(t_m^F\right) \geq \frac{\left(\left(2\tan\left(\alpha_{AV}\left(t_m^F\right)\right) + \tan\left(\alpha_{AV}\left(t_m^S\right)\right)\right)^2 + 6a_{AV}^{MAX}\left(1 + \tan\left(\alpha_{AV}\left(t_m^F\right)\right)\right)^{\frac{3}{2}} y_{AV}\left(t_m^F\right)\right)^{\frac{1}{2}} - \left(2\tan\left(\alpha_{AV}\left(t_m^F\right)\right) + \tan\left(\alpha_{AV}\left(t_m^S\right)\right)\right)}{a_{AV}^{MAX}\left(1 + \tan^2\left(\alpha_m^F\right)\right)^{\frac{3}{2}}} \tag{29}$$

Consequently, to prevent a rollover during lane changing, the lane-changing trajectory's ultimate longitudinal position must satisfy the conditions of Equation (29).

Owing to the intricacies of the actual traffic milieu, it is conceivable that there are either no vehicles or merely one vehicle present in the designated lane. Moreover, the cars in the target lane (TPV, TFV) are likely to execute synchronized lane changes. Our proposed DLCTP model possesses appropriate response capabilities to address these specific scenarios. The sole criterion is the presence or absence of vehicles in the designated lane. If one or two vehicles occupy the target lane, regardless of their actions, appropriate safety limits are computed to guarantee safety. If there is no vehicle on the target lane, the associated safety control will not be executed.

2.5. Final trajectory generation

The cubic polynomial lane-changing trajectory is uniquely defined by the ultimate longitudinal location of the AV, as stated in Sections 2.3 and 2.4 For safety considerations, the ultimate longitudinal position of the AV must fall within the designated safety position range (Equation (27) and Equation (29)). Should the present velocity of the AV satisfy this criterion, the cost function in Equation (21) is computed to determine the ideal trajectory by modifying the parameters (v_{AV}, δ). If not, the lane-changing process will be dangerous; the existing traffic conditions are inappropriate for an AV lane change, necessitating an interruption of the lane-changing process. Under this condition, the existing lane is chosen to be a new target, and the AV reverts to the present lane.

2.6. Lane-changing decision

Before conducting the lane-change maneuver, AV should make decision first. The AV lane-changing decision is to decide when and where to begin the lane change. After getting lane-changing commands, our DLCTP model will try to create a path connecting both current and target positions. If the target position can meet the requirements of safety constraints, including collision-avoidance and rollover-avoidance, AV will begin the lane change immediately. Otherwise, AV will adjust its speed in order to find a suitable lane-changing chance in the next time step. As illustrated in Section 2.3, the lane-changing path is decided by the final longitudinal position $x_{AV}(t_m^F)$, vehicle speed $v_{AV}(t_m^S)$, and weight factor δ. By adjusting weight factor δ and combine the states of surrounding HVs, the minimum speed $v_{AV}^{MIN}(t_m^S)$ and maximum speed $v_{AV}^{MAX}(t_m^S)$ that meet lane-changing start requirements are obtained. Compared with the current speed of the AV $v_{AV}(t_m^S)$, there are three possible cases,

(a) If the current speed of the AV meets these requirements, namely, $v_{AV}^{MIN}(t_m^S) \leq v_{AV}(t_m^S) \leq v_{AV}^{MAX}(t_m^S)$. AV will conduct lane change immediately.

(b) If the current velocity of AV is greater than the maximum allowed velocity to begin lane change, namely, $v_{AV}(t_m^S) > v_{AV}^{MAX}(t_m^S)$, AV needs to slow down to meet the speed requirements. During the deceleration, the target deceleration value should be smaller than maximum deceleration b_n^{MAX} to guarantee passenger comfort and avoid potential collisions with the following vehicle on the current lane (CFV). The target speed of AV in time step $m+1$ is,

$$v_{AV}\left(t_{m+1}^S\right) = \begin{cases} v_{AV}^{MAX}\left(t_m^S\right) & \dfrac{v_{AV}^{MAX}\left(t_m^S\right) - v_{AV}\left(t_m^S\right)}{t_{m+1}^S - t_m^S} \geq -b \\[3ex] v_{AV}\left(t_m^S\right) + b\left(t_{m+1}^S - t_m^S\right) & \dfrac{v_{AV}^{MAX}\left(t_m^S\right) - v_{AV}\left(t_m^S\right)}{t_{m+1}^S - t_m^S} < -b \end{cases}, \forall m \in M, t \in T. \quad (30)$$

(c) If AV's velocity is smaller than the minimum allowed velocity for lane change, namely, $v_{AV}(t_m^S) < v_{AV}^{MIN}(t_m^S)$, AV needs to accelerate to meet the speed requirements. AV should keep a safe time headway with its preceding vehicle on the current lane (CPV) during

the acceleration. The linearized car-following model is employed to guarantee safety with CPV [35].

$$\hat{a}_{\text{CPV}}\left(t_m^{\text{S}}\right) = k_4\left(x_{\text{CPV}}\left(t_m^{\text{S}}\right) - x_{\text{AV}}\left(t_m^{\text{S}}\right) - C - v_{\text{AV}}\left(t_m^{\text{S}}\right)g\right) + k_5\left(v_{\text{CPV}}\left(t_m^{\text{S}}\right) - v_{\text{AV}}\left(t_m^{\text{S}}\right)\right) \tag{31}$$
$$,\forall m \in M, t \in T.$$

And, the target speed of AV in time step $m+1$ is,

$$v_{\text{AV}}\left(t_{m+1}^{\text{S}}\right) = \begin{cases} v_{\text{AV}}^{\text{MIN}}\left(t_m^{\text{S}}\right) & \dfrac{v_{\text{AV}}^{\text{MIN}}\left(t_m^{\text{S}}\right) - v_{\text{AV}}\left(t_m^{\text{S}}\right)}{t_{m+1}^{\text{S}} - t_m^{\text{S}}} \leq \hat{a}_{\text{CPV}} \\[4mm] v_{\text{AV}}\left(t_m^{\text{S}}\right) + \hat{a}_{\text{CPV}}\left(t_{m+1}^{\text{S}} - t_m^{\text{S}}\right) & \dfrac{v_{\text{AV}}^{\text{MIN}}\left(t_m^{\text{S}}\right) - v_{\text{AV}}\left(t_m^{\text{S}}\right)}{t_{m+1}^{\text{S}} - t_m^{\text{S}}} > \hat{a}_{\text{CPV}} \end{cases} ,\forall m \in M, t \in T. \tag{32}$$

By repeating the velocity adjustment process, AV is able to obtain a suitable chance for conducting lane change in the future time step.

3. Simulations and results analysis

3.1. Simulation settings

This section delineates the specific configurations of the simulation, encompassing the software platform, road geometry, traffic scenarios, and essential factors employed in the simulation.

The simulation environment utilized to validate the proposed DLCTP model consists of MATLAB 9.0 and CarSim 2019. The comprehensive simulation process is illustrated in Figure 4; the proposed model operates on MATLAB and transmits the findings to CarSim to control virtual vehicles utilizing a complicated vehicle model. The real-time states (position, heading, speed, acceleration) of all simulation cars are relayed from CarSim to MATLAB, creating a cyclical data flow. Trajectory tracking is not addressed in this study, as it is not the focus of our research. Research on model-predictive-control-based trajectory tracking can be referenced in the works of Raffo *et al.* and Ji *et al.* [36,37]. According to the actual road data from Google Maps, the uninterrupted curved road is depicted in Figure 4. The traffic states are incorporated into the digital map to assess the efficacy of the proposed approach in managing various route geometries. Five vehicles, comprising four heavy vehicles and one AV, are utilized in the scenario. Both the TPV and CPV function in accordance with the established speed and trajectory, whereas other vehicles adhere to the linearized car-following model [35].
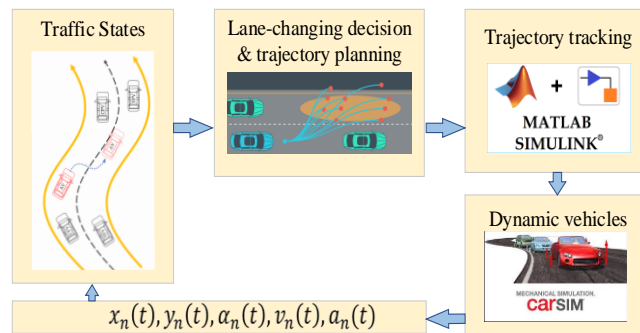

Figure 4. Overall architecture of the simulation platform.

Three representative traffic situations, incorporating various driving behaviors of adjacent high-velocity vehicles, are formulated to assess the adaptability of our model.

(a) The AV transitions from a slow-moving lane to a fast-moving one. The speed of the CPV is less than that of the TPV. This configuration seeks to replicate the AV's pursuit of a sluggishly advancing vehicle, intending to achieve a velocity advantage via lane-changing maneuvers (e.g., circumventing traffic congestion or enhancing driving speed).

(b) The AV executes a lane change between two lanes of comparable speed. Both TPV and CPV maintain a reasonably consistent velocity during the lane-changing maneuver, indicating stable traffic conditions.

(c) The AV changes lanes from a high-speed lane to a low-speed lane. This configuration seeks to replicate the case where AVs must execute obligatory lane changes, such as avoiding obstacles or exiting the road.

The three lane-changing experiment settings account for various traffic situations and driver behaviors in the simulation, facilitating the assessment of the proposed DLCTP model's performance.

The essential parameters utilized in the lane-changing simulation experiments are enumerated in Table 2.

Table 2. Parameters for simulation experiments.

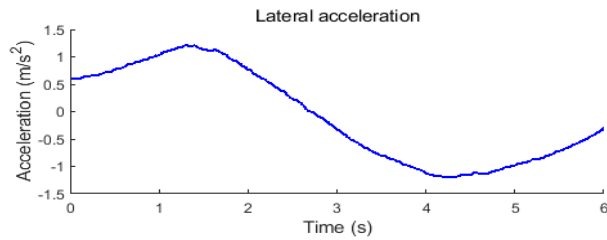| Parameter	Value	Unit
C	4.9	m
a_n^{MAX}	1.4	m/s^2
b_n^{MAX}	-2.8	m/s^2
τ_n	0.9	s
k_4	0.24	s^{-2}
k_5	0.08	s^{-1}
g	1.3	s

3.2. Results analysis
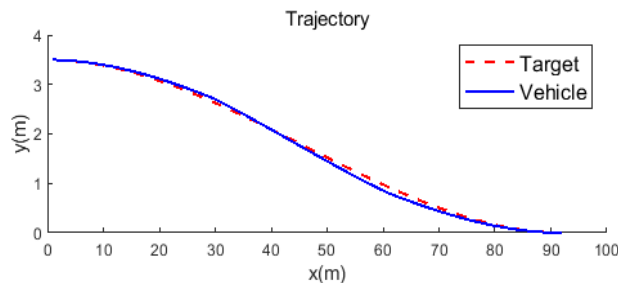
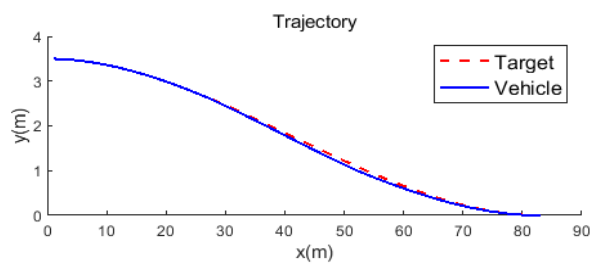

(a) Planned and executed trajectories.
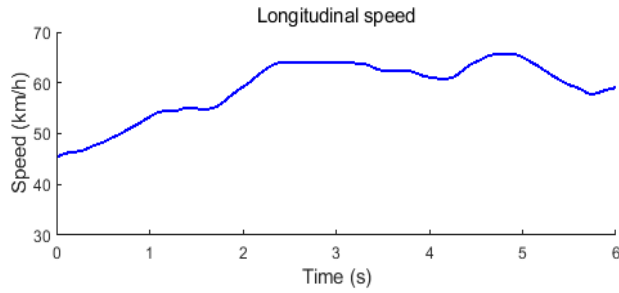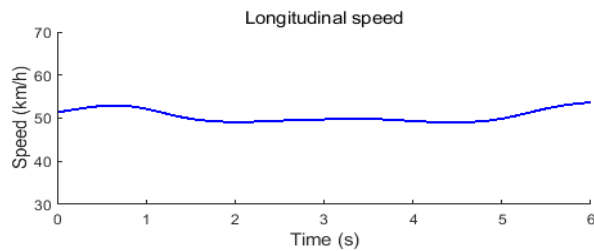
(b) Longitudinal speed.

(c) Lateral acceleration.

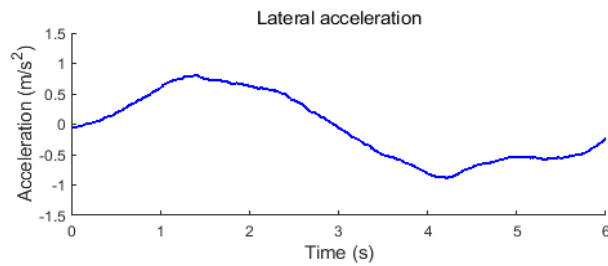**Figure 5.** Simulation results of the acceleration scenario.

Figure 5a illustrates the intended trajectory (red dashed line) and the actual trajectory executed by the vehicle (blue line) within the simulation of the initial traffic scenario. Throughout the lane-changing maneuver, the intended trajectory remains smooth and continuous. The AV demonstrates high-precision trajectory tracking based on this planned path. Both the speed and lateral acceleration of the AV are consistently smooth during the lane change. As depicted in Figure 5b, the AV experiences a comfortable acceleration throughout the experiments. Furthermore, Figure 5c shows that the maximum lateral acceleration during the entire maneuver remains within a comfortable range, ensuring passenger comfort.
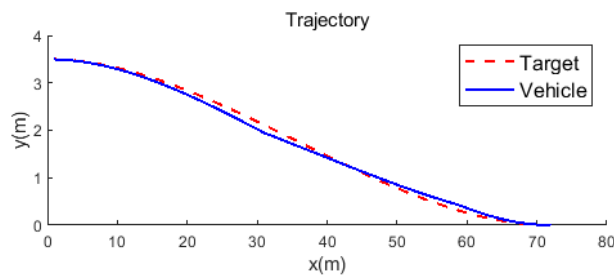

(a) Planned and executed trajectories.
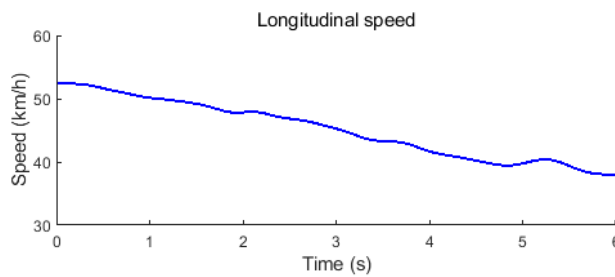

(b) Longitudinal speed.

(c) Lateral acceleration.

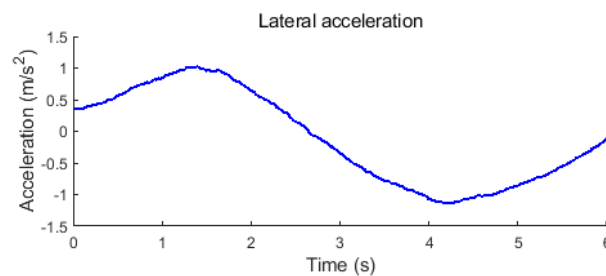**Figure 6.** Simulation results of the const speed scenario.

In the second lane-changing situation, the statuses of adjacent HVs are rather steady. Consequently, there are no significant alterations between two contiguous trajectory plans. The AV can complete the lane-changing maneuver with reduced trajectory tracking error, speed variance, and lateral acceleration. In the constant speed lane change situation, the lateral acceleration is comparatively lower than in the acceleration and deceleration lane change scenario.

(a) Planned and executed trajectories

(b) Longitudinal speed

(c) Lateral acceleration

Figure 7. Simulation results of the deceleration scenario.

Figure 7a demonstrates that the AV can change lane in a deceleration condition with a smooth trajectory and an acceptable trajectory tracking error. The velocity of the AV consistently diminishes throughout the lane shift (shown in Figure 7b), but the lateral acceleration remains acceptable (depicted in Figure 7c).

Our proposed DLCTP model can construct a secure route within 100 milliseconds at each time step throughout the simulation (i7-4710 MQ, 16GB memory, 512GB data storage), indicating the model's decreased resource usage.

The experimental results demonstrate that our proposed DLCTP model can successfully execute safe and comfortable lane-changing operations on curved roads across various traffic circumstances, including both acceleration and deceleration, as well as differing driver behaviors.

4. Conclusion and future work

This paper contributes to the AV's lane-changing trajectory planning in the mixed traffic scenario. The cubic polynomial is utilized in our DLCTP model because to its smoothness and ease of computing. The proposed DLCTP model comprehensively accounts for the dynamics of surrounding high-velocity vehicles and is applicable on both straight and curved roadways. Safety limitations, such as collision avoidance and rollover prevention, are implemented to guarantee the safety, comfort, and efficacy of the lane-changing procedure. A CarSim-Simulink simulation and three representative traffic scenarios are developed and executed to test our proposed DLCTP model. Experimental findings indicate that the proposed DLCTP model can effectively manage intricate traffic situations, encompassing acceleration, constant speed, and deceleration lane changes, while producing a safe, smooth, and efficient trajectory across all three traffic scenarios. Our proposed DLCTP model exhibits reduced usage and is directly applicable in real AV operations.

This research can be expanded in other avenues. Initially, the diverse driving behaviors of heavy vehicles must be considered while formulating the safety limitations. Additionally, field studies must be conducted to validate the DLCTP model.

Acknowledgments

Authors' contribution

Conceptualization, Zhen Wang; data curation and investigation, Jianquan Chen, Pengchao Liu; formal analysis, Pengchao Liu, Bo Dai; writing—original draft preparation, Zhen Wang, Jianquan Chen. All authors reviewed the results and approved the final version of the manuscript.

References

[1] Knoop VL, Buisson C. Calibration and Validation of Probabilistic Discretionary Lane-Change Models. *IEEE Trans. Intell. Transp. Syst.* 2015, 16(2):834–843.

[2] Zheng H, Zhou J, Shao Q, Wang Y. Investigation of a longitudinal and lateral lane-changing motion planning model for intelligent vehicles in dynamical driving environments. *IEEE Access* 2019, 7:44783–44802.

[3] Wang Z, Shi X, Li X. Review of Lane-Changing Maneuvers of Connected and Automated Vehicles: Models, Algorithms and Traffic Impact Analyses. *J. Indian Inst. Sci.* 2019, 99: 589–599.

[4] Yu Q, Zhou Y. Traffic safety analysis on mixed traffic flows at signalized intersection based on Haar-Adaboost algorithm and machine learning. *Saf. Sci.* 2019, 120:248–253.

[5] Zhu WX, Zhang HM. Analysis of mixed traffic flow with human-driving and autonomous cars based on car-following model. *Physica A* 2018, 496:274–285.

[6] Wang Z, Zhao X, Xu Z, Li X, Qu X. Modeling and field experiments on autonomous vehicle lane changing with surrounding human-driven vehicles. *Comput.-Aided Civ. Infrastruct. Eng.* 2021, 36(7):877–889.

[7] Wang Z, Shi X, Zhao X, Li X. Modeling decentralized mandatory lane change for connected and autonomous vehicles: An analytical method. *Transp. Res. Part C Emerg. Technol.* 2021, 133:103441.

[8] Rahman M, Chowdhury M, Xie Y, He Y. Review of Microscopic Lane-Changing Models and Future Research Opportunities. *IEEE Trans. Intell. Transp. Syst.* 2013, 14(4):1942–1956.

[9] Li X, Sun JQ. Studies of vehicle lane-changing dynamics and its effect on traffic efficiency, safety and environmental impact. *Physica A* 2017, 467:41–58.

[10] Wang Z, Zhao X, Chen Z, Li X. A dynamic cooperative lane-changing model for connected and autonomous vehicles with possible accelerations of a preceding vehicle. *Expert Syst. Appl.* 2021, 173:114675.

[11] Peng T, Su L, Zhang R, Guan Z, Zhao H, *et al.* A new safe lane-change trajectory model and collision avoidance control method for automatic driving vehicles. *Expert Syst. Appl.* 2020, 141:112953.

[12] Luo Y, Xiang Y, Cao K, Li K. A dynamic automated lane change maneuver based on vehicle-to-vehicle communication. *Transp. Res. Part C Emerg. Technol.* 2016, 62:87–102.

[13] Nie J, Zhang J, Ding W, Wan X, Chen X, *et al.* Decentralized Cooperative Lane-Changing Decision-Making for Connected Autonomous Vehicles. *IEEE Access* 2016, 4:9413–9420.

[14] Zheng Z. Recent developments and research needs in modeling lane changing. *Transp. Res. Part B Methodol.* 2014, 60:16–32.

[15] Xing Y, Lv C, Wang H, Wang H, Ai Y, *et al.* Driver Lane Change Intention Inference for Intelligent Vehicles: Framework, Survey, and Challenges. *IEEE Trans. Veh. Technol.* 2019, 68(5):4377–4390.

[16] Gipps PG. A model for the structure of lane-changing decisions. *Transp. Res. Part B Methodol.* 1986, 20(5):403–414.

[17] Ma Y, Zhang P, Hu B. Active lane-changing model of vehicle in B-type weaving region based on potential energy field theory. *Physica A* 2019, 535: 122291.

[18] Yu H, Tseng HE, Langari R. A human-like game theory-based controller for automatic lane changing. *Transp. Res. Part C Emerg. Technol.* 2018, 88:140–158.

[19] Ali Y, Zheng Z, Haque MM, Wang M. A game theory-based approach for modelling mandatory lane-changing behaviour in a connected environment. *Transp. Res. Part C Emerg. Technol.* 2019, 106:220–242.

[20] Toledo T, Koutsopoulos HN, Ben-Akiva M. Integrated driving behavior modeling. *Transp. Res. Part C Emerg. Technol.* 2007, 15(2):96–112.

[21] Yang D, Zhu L, Ran B, Pu Y, Hui P. Modeling and Analysis of the Lane-Changing Execution in Longitudinal Direction. *IEEE Trans. Intell. Transp. Syst.* 2016, 17(10):2984–2992.

[22] Suh J, Chae H, Yi K. Stochastic Model-Predictive Control for Lane Change Decision of Automated Driving Vehicles. *IEEE Trans. Veh. Technol.* 2018, 67(6):4771–4782.

[23] Zhang Y, Gao B, Guo L, Guo H, Cui M. A Novel Trajectory Planning Method for Automated Vehicles under Parameter Decision Framework. *IEEE Access* 2019, 7:88264–88274.

[24] Kesting A, Treiber M, Helbing D. General lane-changing model MOBIL for car-following models. *Transp. Res. Rec.* 2007, 1991(1):86–94.

[25] He J, He Z, Fan B, Chen Y. Optimal location of lane-changing warning point in a two-lane road considering different traffic flows. *Physica A* 2020, 540:123000.

[26] Liu Y, Wang X, Li L, Cheng S, Chen Z. A Novel Lane Change Decision-Making Model of Autonomous Vehicle Based on Support Vector Machine. *IEEE Access* 2019, 7:26543–26550.

[27] Hou Y, Edara P, Sun C. Situation assessment and decision making for lane change assistance using ensemble learning methods. *Expert Syst. Appl.* 2015, 42(8):3875–3882.

[28] Tang J, Liu F, Zhang W, Ke R, Zou Y. Lane-changes prediction based on adaptive fuzzy neural network. *Expert Syst. Appl.* 2018, 91:452–463.

[29] Ye Y, Zhang X, Sun J. Automated vehicle's behavior decision making using deep reinforcement learning and high-fidelity simulation environment. *Transp. Res. Part C Emerg. Technol.* 2019, 107:155–170.

[30] Dabeer O, Ding W, Gowaiker R, Grzechnik SK, Lakshman MJ, *et al.* An end-to-end system for crowdsourced 3D maps for autonomous vehicles: The mapping component. In *IEEE/RSJ International Conference on Intelligent Robots and Systems (IROS)*, Vancouver, Canada, 24–28 September 2017, pp. 634–641.

[31] Urmson C, Anhalt J, Bagnell D, Baker C, Bittner R, *et al.* Autonomous Driving in Urban Environments: Boss and the Urban Challenge. *J. Field Robot.* 2008, 25(8): 425–466.

[32] Yang D, Zheng S, Wen C, Jin PJ, Ran B. A dynamic lane-changing trajectory planning model for automated vehicles. *Transp. Res. Part C Emerg. Technol.* 2018, 95:228–247.

[33] Benloucif MA, Popieul JC, Sentouh C. Multi-level cooperation between the driver and an automated driving system during lane change maneuver. In *2016 IEEE Intelligent Vehicles Symposium (IV),* Gothenburg, Sweden, 19–22 June 2016, pp. 1224–1229.

[34] Ross M, Patel D, Wenzel T. Vehicle design and the physics of traffic safety. *Phys. Today* 2006, 59(1):49–54.

[35] Milanés V, Shladover SE. Modeling cooperative and autonomous adaptive cruise control dynamic responses using experimental data. *Transp. Res. Part C Emerg. Technol.* 2014, 48:285–300.

[36] Raffo GV, Gomes GK, Normey-Rico JE, Kelber CR, Becker LB. A predictive controller for autonomous vehicle path tracking. *IEEE Trans. Intell. Transp. Syst.* 2009, 10(1):92–102.

[37] Ji J, Khajepour A, Melek WW, Huang Y. Path planning and tracking for vehicle collision avoidance based on model predictive control with multiconstraints. *IEEE Trans. Veh. Technol.* 2016, 66(2):952–964.